Mechanism of Charge Separation and Stabilization of Separated Charges in Reaction Centers of *Chloroflexus aurantiacus* and of YM210W(L) Mutants of *Rhodobacter sphaeroides* Excited by 20 fs Pulses at 90 K[†]

A. G. Yakovlev,[‡] L. G. Vasilieva,[§] A. Ya. Shkuropatov,[§] T. I. Bolgarina,[§] V. A. Shkuropatova,[§] and V. A. Shuvalov[‡,§,*]

Department of Photobiophysics, Belozersky Institute of Chemical and Physical Biology, Moscow State University, Moscow 119992, Russia, and Institute of Basic Biological Problems, Russian Academy of Sciences, Pushchino, Moscow Region 142290, Russia

Received: January 16, 2003; In Final Form: June 5, 2003

The nuclear wave packet formed by 20 fs excitation on the P* potential energy surface in native and mutant (YM210W and YM210L) reaction centers (RCs) of *Rhodobacter (Rb.) sphaeroides* and in *Chloroflexus (C.) aurantiacus* RCs was found to be reversibly transferred to the $P^+B_A^-$ surface at 120, 380, etc. fs delays (monitored by measurements of B_A^- absorption at 1020−1028 nm). The YM210W(L) mutant RCs show the most simple pattern of femtosecond oscillations with a period of 230 fs in stimulated emission from P* and with the initial amplitude comparable to that in plant pheophytin *a* (Pheo)-modified *Rb. sphaeroides* R-26 RCs. Similar reversible oscillations are observed in the 1020 nm band of the mutants, the initial amplitude of which is smaller by a factor of ∼10 with respect to Pheo-modified *Rb. sphaeroides* R-26 RCs. In contrast to native and Pheo-modified *Rb. sphaeroides* R-26 RCs, irreversible quasi-exponential stabilization of $P^+B_A^-$ is considerably suppressed in the mutant RCs in the picosecond time domain. The water rotational mode with a frequency of 32 cm^{-1} and its overtones, described earlier (Yakovlev; et al. *Biochemistry* **2002,** *41,* 2667−2674), are decreased in the YM210W(L) mutants and strongly suppressed in dry films of the mutant RCs. In the dry film of both YM210W and YM210L RCs neither reversible nor irreversible $P^+B_A^-$ formation monitored at 1020 nm is observed despite the preservation of fs oscillations with a frequency of 144 cm^{-1} in the 935 nm kinetics of stimulated emission from P*. Furthermore, the 1020 nm band is not formed inside of P*. In *C. aurantiacus* RCs, containing leucine instead of tyrosine at the M208 position, the P* decay is slowed to ∼5 ps at 90 K (1.5 ps in *Rb. sphaeroides* RCs) and characterized by fs oscillations with the amplitude comparable to that measured in native *Rb. sphaeroides* R-26 RCs. The B_A^- absorption band development at 1028 nm is observed at 90 K with fs oscillations similar to those described for native *Rb. sphaeroides* R-26 RCs at 293 K but with the amplitude being smaller by a factor of ∼6. The kinetics of absorbance changes in the 1028 nm band in *C. aurantiacus* RCs includes the stabilization of $P^+B_A^-$ within ∼5 ps with subsequent decay due to electron transfer to H_A within ∼1 ps. The mechanisms of the electron-transfer between P* and B_A and of the stabilization of the state $P^+B_A^-$ in bacterial RCs are discussed.

Introduction

The reaction center (RC) is a pigment protein complex responsible for the light energy conversion into the free energy of the charge separated states in photosynthetic bacteria and green plants. In purple bacteria RCs a local 2-fold rotational axis runs through two strongly interacting bacteriochlorophylls constituting the special pair P near the periplasmic side of the membrane and the Fe atom located between two quinones (Q_A and Q_B) near the cytoplasmic side of the membrane.[1,2] The axis separates symmetrically two bacteriochlorophyll monomers (B_A and B_B) and two bacteriopheophytins (H_A and H_B) located in the hydrophobic central part of the membrane. The quinones (Q_A and Q_B) terminate two branches (A and B) of the chromophores. Light-induced charge separation results in the formation of positive (P^+) and negative (Q^-) charges on opposite

sides of the membrane used for further biochemical processes in the cell. The sequence of the electron-transfer (ET) reactions shows that charge separation takes place in the A branch.[3]

On the basis of time-resolved spectroscopic measurements,[4−13] B_A has been suggested to play the role of the primary electron acceptor in agreement with its position between P and H_A in the X-ray model of RCs.[1,2] The state $P^+B_A^-$ can be a first charge separated state in which radical cation (P^+) and anion (B_A^-) have spectral properties close to those observed individually.

The sum of the experimental data has been interpreted by several groups as an indication of the parallel possibilities for the two-step ET with an electron being transferred to B_A prior H_A, and for the superexchange mechanism involving the vacant orbital of B_A for ET from P* to H_A.[14−20]

Recently the formation of the long-lived (∼1 ns) state $P^+B_A^-$ has been observed in Pheo-modified *Rb. sphaeroides* R-26 RCs in which the interaction between P and B_A remained to be unchanged but ET to H_A was blocked by pigment exchange. The state $P^+B_A^-$ was observed with spectral properties close to the sum of those for P^+ and B_A^-.[6,8,9] The 1020 nm absorption

Separated Charges in *C. aurantiacus* and *Rb. sphaeroides*

J. Phys. Chem. A, Vol. 107, No. 40, 2003 **8331**

band registered for this state was found to be characteristic for the radical anion of bacteriochlorophyll. As shown in ref 21, the appearance of the 1020 nm band at a very early time (at 120 fs) after excitation of P strongly suggests that the state $P^+B_A^-$ is a first product of the charge separation. It has also been found[9] that in Pheo-modified RCs the B_A band bleaching at 800 nm corresponds stoichiometrically to the P band bleaching at 890 nm. The amplitude of the P band bleaching is not changed when P^*B_A is converted to $P^+B_A^-$ within 1.5 ps. This fact indicates that all electron density is shifted from P* to B_A in the picosecond time domain. Furthermore, it was shown that $P^+B_A^-$ has lower energy than P*, and that very little admixture of superexchange is present in bacterial RCs (see ref 9 for references therein).

The mutual arrangement of P_A, P_B, and B_A determined by X-ray analysis in great detail[1,2] shows several possibilities for the ET pathway from P* to B_A. To study these possibilities, femtosecond (fs) coherent spectroscopy and the frequency analysis of vibration and rotation of the molecular groups involved in charge separation have recently been applied.[21-29] This approach in combination with site-directed mutagenesis of the RC protein offers an opportunity to address the problem of stabilization of separated charges as well.

Excitation of P by ultrashort (<30 fs) pulses of a broad spectral width creates a superposition of several vibrational wave functions known as a wave packet. The wave packet has a time dependent position on the potential energy surface of P* and moves with the frequency corresponding to the energy difference between the vibrational levels involved. Such nuclear wave packet motions were first visualized by measurements of the fs oscillations in the kinetics of stimulated emission from P*.[22-25] A displacement of the potential energy surface of P* with respect to that of P results in the time dependent spectral position of the wave packet stimulated emission from P*. The long- and short-wavelength emission components are out of phase with each other but have similar oscillation frequencies. It has been shown that the motion of the wave packet to the long-wavelength emission region on the P* potential energy surface is accompanied by the reversible electron transfer from P* to B_A with a formation of the 1020 nm absorption band of B_A^-, the initial period being of about 260 fs both at 293 K[21,27-29] and 90 K.[26] This observation indicates that the long-wavelength wave packet position is near the intercrossing point between the P* and $P^+B_A^-$ surfaces.

On the basis of the results of DOH(DOD)/HOH exchange in a buffer solution and measurements in dry films of *Rb. sphaeroides* R-26 RCs, the 32 cm^{-1} fundamental mode and its overtones, observed in the kinetics of the 1020 nm band of B_A^- and of the 935 nm stimulated emission from P*, has been suggested to be related to the rotation of the water molecule.[26] This assumption is consistent with the gas-phase specific frequencies of HOH rotation at 20, 32, and 52 cm^{-1}. The 32 cm^{-1} mode was shown to modulate the electron transfer from P* to B_A in at least 35% of RCs. It has been proposed therefore that one of the molecular pathways for the electron transfer from P* to B_A in *Rb. sphaeroides* RCs might be along the bridge formed by polar groups according to the Brookhaven Protein Data Bank (1AIJ): $Mg(P_B)-N-C-N(His M202)-HOH(55)-O=(B_A)$. (In the very similar structure of *Rps. viridis* RCs the homologous water molecule is numbered as HOH302 (1PRC)). In this context, a study of the mutant RCs having specific amino acid substitutions near the possible ET pathway is of great interest.

The first approaches of the wave packet to the intercrossing area between the P* and $P^+B_A^-$ potential energy surfaces at 120 and 380 fs lead to a partial stabilization of the separated charges in the state $P^+B_A^-$, which stabilization is completed within ~1.5 ps in Pheo-modified and native RCs at 90 K.[26] The process seems to be modulated by the 32 cm^{-1} mode and its overtones. The subsequent electron transfer from B_A^- to H_A in native RCs proceeds within ~300 fs at 90 K and ~1000 fs at 293 K and is accompanied by decay of the 1020 nm band of B_A^-.[5,7,8,10-13,21,26] The mechanism of the stabilization process is not yet completely clear. One possibility can be related to a reorientation of the polar groups of the amino acid residues located near P and B_A. Such a group might be represented by the OH group of tyrosine located at the position M210 in the vicinity of P and B_A in *Rb. sphaeroides* RCs (M208 in *Rps. viridis* and *Chloroflexus aurantiacus* RCs).[1,2]

In the present report we examine a role of tyrosine M210 in the charge separation and stabilization of separated charges by studying coherent fs oscillations in kinetics of decay of stimulated emission from P* and of a population of the primary charge separated state $P^+B_A^-$ in the mutant RCs of *Rb. sphaeroides* in which the tyrosine M210 has been replaced by a tryptophan (YM210W) or by a leucine (YM210L). In addition, the measurements were also carried out on RCs of the thermophilic green bacterium *Chloroflexus (C.) aurantiacus* containing leucine at the analogous position M208 (see refs 30-37).

RCs of the genetically engineered mutants YM210W and YM210L of *Rb. sphaeroides* have carefully been investigated in many respects, including the X-ray crystal structure, redox properties of P, the rates of ET reactions, etc.[35,38-43] In YM210W the redox potential of P$^+$/P lies approximately 55 mV above that in WT RCs.[42] The free energy gap between P* and $P^+H_A^-$ is diminished by ~60 mV.[39] The lifetime of P* is increased from 3 to 4 ps in WT to several tens of picoseconds in the mutants.[38-42] It is interesting that in the YM210W mutant a newly introduced tryptophan molecule appears to cause a small tilt of the B_A macrocycle, mainly affecting the positions of the rings II and III.[43] This change in the geometry of B_A can probably change a position of the HOH55 water molecule. The situation might be different in the YM210L mutant because a volume of leucine is less than that of tyrosine.

Another example of the influence of the amino acid residue at the position M210 (M208) on charge separation is presented by RCs of *C. aurantiacus*. This type of RCs shows ET kinetics[30-37] significantly different from that in native *Rb. sphaeroides* RCs. More specifically, the initial charge separation step is slowed to 7 ps at 296 K. At 10 K, two components for the P* decay were observed with the time constants of 2 and 24 ps. By analogy to the YM210L mutant RCs of *Rb. sphaeroides*, a decreased rate of charge separation in *C. aurantiacus* RCs can be explained by the presence of leucine at the position M208 (instead of TyrM210 in native *Rb. sphaeroides* RCs). Note, however, that there are other differences between *Rb. sphaeroides* and *C. aurantiacus* RCs, both in the pigment and protein composition. With regard to the mechanism of charge separation and stabilization, the interesting difference is the presence of another tyrosine residue in *C. aurantiacus* RCs, located close to P at the position M195. Significant ET along the B-branch of pigments has been proposed for *C. aurantiacus* RCs.

Here we show that the mutant YM210W and YM210L RCs of *Rb. sphaeroides* exhibit the simplest pattern of fs oscillations. The seven periods of the oscillation are clearly seen in the 935

nm kinetics as well as in the 1020 nm kinetics (amplitude is decreased by a factor of ∼10 with respect to native RCs). The modulation by the 32 cm^{-1} fundamental mode is considerably weaker in the mutant RCs with respect to that observed in native and pheophytin-modified RCs of *Rb. sphaeroides* R-26.[26] The overtones of the 32 cm^{-1} mode are partially present in the mutant RCs suspended in a water buffer but disappear in their dry films. No ET from P* to B_A with a formation of the 1020 nm band is observed in dry films. The quasi-exponential stabilization of $P^+B_A^-$ is considerably suppressed in hydrated YM210W and YM210L mutants. In *C. aurantiacus* RCs the 190 fs oscillation is observed at 90 K modulated by the modes at 35 and 52 cm^{-1}. The quasi-exponential stabilization of $P^+B_A^-$ occurs within ∼5 ps at 90 K with subsequent ET from B_A^- to H_A within ∼1 ps. These data are discussed in terms of the mechanism of the charge separation and stabilization of the separated charges in the state $P^+B_A^-$. The model for dynamic stabilization of separated charges by means of reorientation of the OH group of YM210 in *Rb. sphaeroides* and of YM195 in *C. aurantiacus* located in the vicinity of P and B_A is proposed.

Materials and Methods

The mutations YM210W and YM210L were introduced in pufM gene encoding M protein subunit of the reaction center of *Rb. sphaeroides* using bacterial strains and plasmids, as described in ref 44. Mutant RCs as well as RCs of *Rb. sphaeroides* R-26 and *C. aurantiacus* were isolated by treatment of membranes with LDAO followed by DEAE-cellulose chromatography.[30] Both native bacteriopheophytins (H_A and H_B) were exchanged in *Rb. sphaeroides* R-26 RCs with plant pheophytin *a* (Pheo) according to refs 6, 8, and 45.

For studies at room-temperature RCs were suspended in 10 mM Tris−HCl, pH 8.0/0.1% Triton-X100 buffer (TT buffer). Low-temperature (90 K) measurements were performed on the samples containing 65% glycerol (v/v). The optical density of the samples was 0.5 at 860 nm at room temperature. Sodium dithionite (5 mM) was added to keep RCs in the state $PB_AH_AQ_A^-$.

A dry film of RCs was obtained by drying of the RCs solution at room temperature and relative humidity of ∼40% and then under vacuum conditions for 2 days. Before measurements the film was illuminated by 1064 nm laser microsecond pulses to evaporate residual water molecules. The absorption spectrum of RCs in the dry film was different from that in liquid by a ∼7 nm blue shift of the Q_Y band of P with a preservation of the Q_Y band of B_A.

Femtosecond transient absorption measurements were carried out with a Tsunami Ti:sapphire fs laser pumped by Millennia YAG laser (both Spectra Physics, USA). The fs pulses were amplified by a home-built Ti:sapphire amplifier followed by a continuum generator, pump−probe scheme and an optical multichannel analyzer, described earlier in detail.[28] The operating frequency was 15 Hz. The duration of pump and probe pulses was about 20 fs. Spectrally broad pump pulses were centered at 870 nm. The delay between pump and probe pulses was changed with an accuracy of ∼10 fs. The spectral band of the green glass filter (ZC-10, LOMO, St.-Petersburg) in the range 900−1060 nm was found to bleach within 30 fs without any changes of the shape of the band. This indicates that the temporal dispersion in this spectral region was compressed to less than 30 fs.

Transient absorption difference spectra were obtained by averaging of 7000−10000 measurements at each time delay. The accuracy of absorbance measurements was $(1-3) \times 10^{-5}$
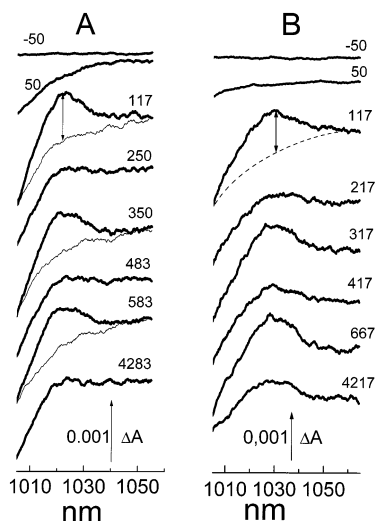

Figure 1. Difference (light-minus-dark) absorption spectra in the range 1000−1060 nm acquired at various fs delays at 90 K in mutant YM210W RCs of *Rb. sphaeroides* (A) and in *C. aurantiacus* (B) RCs in glycerol-TT buffer (thick curves) and in dry film of the mutant RCs where the formation of the 1020 nm is absent (thin curves in A show the 1020 nm region for delays at 117, 350, and 583 fs). RCs were excited by 20 fs pulses at 870 nm. The double arrows show amplitudes of the absorbance changes (ΔA) for spectral bands at 1020 and 1028 nm superimposed on the broad spectral background. These amplitudes were used for the kinetics plots presented in Figures 2, 4, and 6. The same was done (data not shown) for the stimulated emission band at 935 nm (see Figures 3 and 5).

units of optical density. The amplitude of the spectral bands at 1020−1028 and 935 nm (not shown) at different delays superimposed on the broad background was measured at their maxima, as shown by double arrows in Figure 1. The kinetics of absorbance changes (ΔA) at 1020−1028 and 935−945 nm were plotted using the measured amplitudes. The polynomial nonoscillating fits were found mathematically and subtracted from the kinetics. The residual oscillatory parts of the kinetics were Fourier transformed (FT) to obtain the frequency spectra of oscillations. The fits correspond to minimal noise in FT spectra and to minimal amplitude of the oscillations. This approach seems to be more appropriate because there is a large contribution from adiabatic processes to ET under 20 fs excitation. Uncertainty of the FT peaks is caused by an ordinate noise, the level of which is clearly seen for each spectrum.[26] The abscissa uncertainty of ±4 cm^{-1} is related to the width of the measurement window (4.3 ps). Because the oscillations disappear within this time the artificial increase of the window (additional zero points after 4.3 ps) would not change experimental data but decrease the abscissa uncertainty. This approach has shown that the position of the major peaks is preserved in FT spectra.

Results

Figure 1 shows the spectra of absorbance changes (ΔA) measured in RCs of the *Rb. sphaeroides* mutant YM210W (A) and of *C. aurantiacus* (B) at different fs delays at 90 K in the range from 1000 to 1060 nm where the formation of the B_A^- absorption band is expected to be observed. The difference absorption spectra for the YM210L mutant of *Rb. sphaeroides* (not shown) were very similar to those found for YM210W both in shape and amplitude. The double arrows show the amplitudes of the bands at 1020 nm (YM210W) and at 1028 nm (*C. aurantiacus*) used for plotting the kinetics of population of the state $P^+B_A^-$ presented in Figures 2, 4, and 6. The same
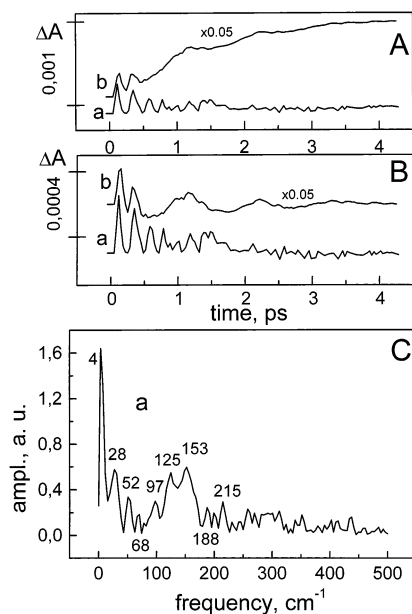
Separated Charges in *C. aurantiacus* and *Rb. sphaeroides*

J. Phys. Chem. A, Vol. 107, No. 40, 2003 **8333**

Figure 2. Femtosecond kinetics of ΔA (A), its oscillatory part (B), and the spectrum of the Fourier transform of the oscillatory part (C) for the 1020 nm band in mutant YM210W (a) and pheophytin-modified (b) RCs of *Rb. sphaeroides* in glycerol-TT buffer at 90 K. RCs were excited by 20 fs pulses at 870 nm. The data for pheophytin-modified R-26 RCs are taken from ref 26.
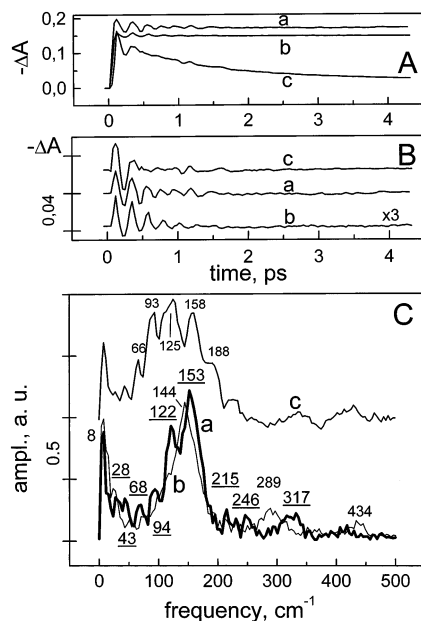

Figure 4. Femtosecond kinetics of ΔA (A), its oscillatory part (B), and the spectrum of the Fourier transform of the oscillatory part (C) for the 1020 nm band in mutant YM210L RCs of *Rb. sphaeroides* at 90 K. Glycerol-TT buffer was used. RCs were excited by 20 fs pulses at 870 nm.

Figure 3. Femtosecond kinetics of ΔA (A), its oscillatory part (B), and the spectrum of the Fourier transform of the oscillatory part (C) for the 935 nm band in mutant YM210W (a and b) and pheophytin-modified (c) RCs of *Rb. sphaeroides* in glycerol-TT buffer (a and c) and in dry film (b) at 90 K. RCs were excited by 20 fs pulses at 870 nm. Underscored numbers in C (curve a) show the characteristic frequencies of FT spectra of YM210W RCs in glycerol-TT buffer whereas nonunderscored numbers show the analogous frequencies of RCs in dry film (curve b) and in pheophytin-modified RCs (curve c). The data for pheophytin-modified R-26 RCs are taken from ref 26.

Figure 5. Femtosecond kinetics of ΔA (A), its oscillatory part (B), and the spectrum of the Fourier transform of the oscillatory part (C) for the 935 nm band in the mutant YM210L RCs of *Rb. sphaeroides* in glycerol-TT buffer (thick curves) and in dry film (thin curves) at 90 K. RCs were excited by 20 fs pulses at 870 nm.

procedure was used to obtain the kinetics of decay of the stimulated emission from P* (see Figures 3 and 5) by measuring the amplitude of ΔA near 935−945 nm (data not shown). In Figures 2−6 the kinetics (section A), their oscillatory parts (section B) and Fourier transforms of the oscillatory parts (section C) are shown for the different types of RCs used in this study.
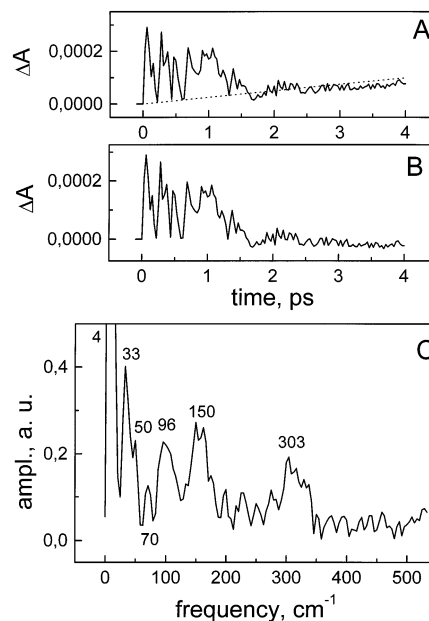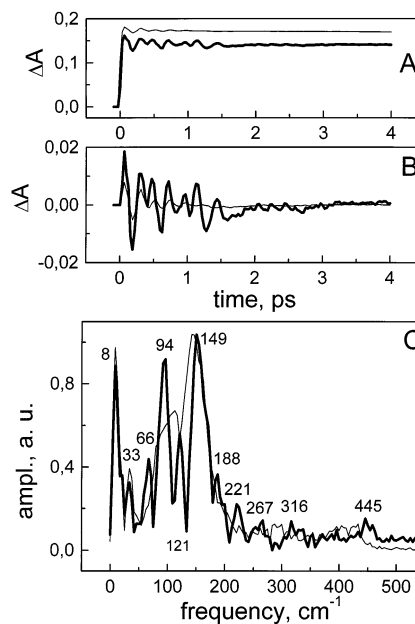
The kinetics at 935 nm measured for the mutants YM210W and YM210L at 90 K are similar to each other and show very slow P* decay in the picosecond time domain (Figures 3 and 5) in agreement with earlier data.[35,38−43] This fact is consistent with almost complete absence of quasi-exponential stabilization of the state $P^+B_A^-$ in the mutant RCs within 4.3 ps. Indeed, the amplitude of the 1020 nm absorption band at 4 ps in both mutants is as low as 0.0001 units of optical density (Figures 2 and 4). For comparison, the absorption at 1020 nm in Pheo-modified RCs approaches a value of ∼0.02 at 4 ps (Figure 2A, curve b). Note that a level of quasi-exponential stabilization of $P^+B_A^-$ (going as a background for coherent oscillations) is
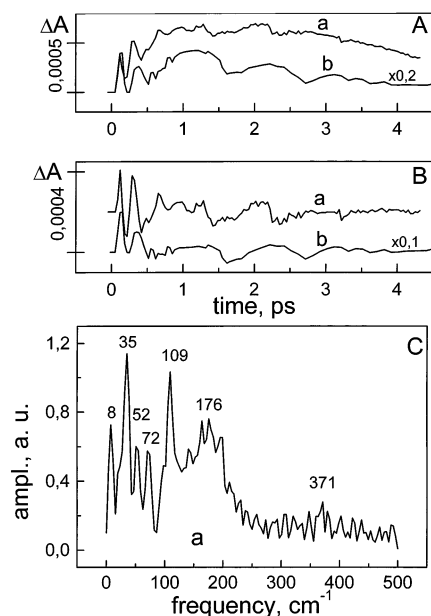
Figure 6. Femtosecond kinetics of ΔA (A), its oscillatory part (B), and the spectrum of the Fourier transform of the oscillatory part (C) for the 1028 nm band in *C. aurantiacus* RCs at 90 K (a) and for the 1020 nm band in native *Rb. sphaeroides* R-26 RCs at 293 K (b). Glycerol-TT buffer was used. RCs were excited by 20 fs pulses at 870 nm. The data for *Rb. sphaeroides* RCs are taken from ref 26.

slightly higher in YM210L than in YM210W (Figures 2A and 4A). This is accompanied by an appearance of the 33 cm^{-1} mode in FT spectrum in YM210L (Figure 4C).

The oscillatory parts of the kinetics at 1020 and 935 nm in the mutant YM210W and YM210L RCs of *Rb. sphaeroides* at 90 K are similar to each other and represent the simplest pattern measured until now[21,26−29] (Figures 2 and 3, curves a; Figures 4 and 5). For comparison the oscillatory parts of the kinetics in Pheo-modified RCs of *Rb. sphaeroides* R-26 are presented in Figure 2 (curves b) and Figure 3 (curves c). The slowly decaying first seven peaks appearing with a period of 230 fs in the 1020 nm kinetics are observed in RCs of the mutants. The initial amplitude of the oscillation is smaller by a factor of ∼10 than that in Pheo-modified RCs (Figure 2). The similar oscillation is seen in the 935 nm kinetics in the mutant RCs (Figures 3 and 5, curves a, b) with the same initial amplitude as in Pheo-modified RCs (Figure 3, curves c). Remarkably that the alike peaks in the 1020 nm kinetics in Pheo-modified and native RCs are modulated by the low-frequency mode at 32 cm^{-1} and its overtones (Figures 2 and 6, curves b). In the mutant YM210W RCs this mode is strongly suppressed, although some overtones of the 31 cm^{-1} mode are discernible in FT spectra for both kinetics at 68, 94−97, 122−125, 153, 188, 215, and 246 cm^{-1} (Figures 2C and 3C, curves a). In the YM210L mutant the mode at 33 cm^{-1} is seen together with other frequencies at 49, 66, 94, 121, 149, 188, 221, 266, 316, and 446 cm^{-1} (Figure 5). Most of these frequencies seem to represent a combination of the ∼32 and ∼49 cm^{-1} modes and their overtones.

The higher overtones are considerably decreased in the kinetics at 935 nm in the dry film of the mutant YM210W RCs (Figure 3, curves b). A single mode at 144 cm^{-1} is only discerned with its overtones at 289 and 434 cm^{-1}. In the dry film of the YM210L mutant RCs the FT spectrum is more complicated (Figure 5) showing some structure of vibrational modes near 112 and 143 cm^{-1}. No formation of the 1020 nm band of B_A^- and consequently no electron transfer from P* to

B_A is registered in the picosecond time domain in YM210W (Figure 1A, thin lines) and YM210L (not shown) under dehydration.

The presence of the 144 cm^{-1} oscillations in the 935 nm kinetics and absence of the B_A^- band formation in dry films of the mutant YM210W demonstrates that the oscillations in the excited dimer P* are independent of ET from P* to B_A. These data suggest that the fs oscillations are generated in the state P* as a result of the motion of the wave packet (probably vibrational) on the P* potential energy surface and that there is no formation of the 1020 nm band inside of P*. The nuclear wave packet motion on the P* surface is accompanied by ET from P* to B_A when the specific conditions for that (optimal energy difference, small tunnel barrier and/or effective ET pathway, etc.) are satisfied. As follows from the absence of the B_A^- absorption at 1020 nm, such conditions are not realized in the dry films of the mutant RCs. One possible interpretation of the effect of dehydration might be related to a removal of HOH55 resulting in blocking the ET pathway via a bridge P−HisM202-HOH−B_A (see ref 26 and Discussion).

In *C. aurantiacus* RCs the decay time of P* at 90 K is about 5 ps (not shown), which is considerably longer than that in native and pheophytin-modified *Rb. sphaeroides* R-26 RCs (∼1.5 ps). The fs oscillations in the 945 nm kinetics of the P* stimulated emission are observed in *C. aurantiacus* RCs, which are similar in shape and amplitude to those found for *Rb. sphaeroides* R-26 RCs. The FT spectrum of the oscillatory part of the 945 nm kinetics in *C. aurantiacus* includes two main bands at 113 and 167 cm^{-1} (not shown). The similar but more clear FT spectrum is revealed for the oscillatory part of the 1028 nm kinetics in *C. aurantiacus* RCs at 90 K, which has a ∼6 times smaller amplitude than that in native *Rb. sphaeroides* RCs (Figure 6). The spectrum includes two fundamental frequencies at 35 and 52 cm^{-1} and frequencies at 72, 109, and 176 cm^{-1}. These latter frequencies can be ascribed to the overtones of the 35 and 52 cm^{-1} modes superimposed on the vibrational mode like that observed in RCs of the YM210L mutant of *Rb. sphaeroides* (Figures 4 and 5).

The quasi-exponential stabilization of $P^+B_A^-$ as a background for coherent oscillations is observed within 1 ps and followed by a decay within ∼5 ps in *C. aurantiacus* RCs at 90 K (Figure 6A, curve a). This complicated kinetics is similar to a slightly faster kinetics at 1020 nm registered in *Rb. sphaeroides* R-26 RCs at 293 K[21] (Figure 6A, curve b) (low-temperature kinetics in R-26 displays even faster decay due to faster ET from B_A^- to H_A[26]). The kinetics at 1028 nm in *C. aurantiacus* corresponds to the 5 ps charge separation between P* and B_A and further ET from B_A^- to H_A within ∼1 ps. The oscillatory parts of the kinetics in both *C. aurantiacus* and *Rb. sphaeroides* RCs show two initial peaks at 120 and 350−380 fs with subsequent low-frequency modulation (Figure 6B). The stabilization of the state $P^+B_A^-$ is accompanied by the coherent modulation by the mode at 35 cm^{-1} in *C. aurantiacus* and at 32 cm^{-1} in *Rb. sphaeroides*[21] RCs.

Discussion

The data presented indicate that the simplest pattern of fs oscillations in the kinetics at 935 and 1020 nm is observed in the mutants YM210W and YM210L of *Rb. sphaeroides* at 90 K (Figures 2−5). In these mutants, decay of the stimulated emission from P* at 935 nm and a stabilization of the state $P^+B_A^-$ is considerably slowed especially at low temperature (up to ∼300 ps at 90 K as compared to ∼1.5 ps in native *Rb. spaeroides* RCs) in agreement with earlier observations.[35,38−43]
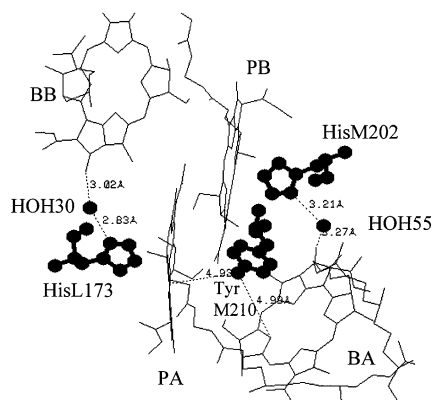
Figure 7. View (Brookhaven Protein Data Bank, 1AIJ) of a special pair of bacteriochlorophylls P_A and P_B (P_L and P_M, respectively), monomeric bacteriochlorophylls B_A and B_B, His M202, His L173, Tyr M210, HOH55, and HOH30 in *Rb. sphaeroides* RCs. Numbers represent the distances in Å. The oxygen of Tyr M210 is located symmetrically between P_A and B_A and separated from C−N(IV) of P_A (positively charged[46]) and from N(II) of B_A (negatively charged) by ∼5 Å. This tyrosine is present in *Rb. sphaeroides* but not in *C. aurantiacus* RCs. In latter RCs there is another tyrosine M195 in the vicinity of P and B_A. The tyrosine at the analogous position is present in RCs of *Rps. viridis* but it is absent in the structure of *Rb. sphaeroides*. According to the atomic coordinates for *Rps. viridis* RCs (Brookhaven Protein Data Bank, 1PRC) the oxygen of TyrM195 is much closer to C−N(II) of P_A (3.78 Å) than to N(II) of B_A (9.05 Å). In *Rb. sphaeroides* RCs the oxygen of HOH55 is separated from the oxygen of the keto carbonyl group of ring V of B_A by 3.27 Å and from the nitrogen of His M202 by 3.21 Å. See text for details.

Notably, even in this case several (∼7) peaks of fs oscillations are observed in both kinetics with a period of ∼230 fs (Figures 2−5).

The higher overtones of the 32 and 50 cm⁻¹ modes with relatively smaller amplitude (as compared to native and pheophytin-modified RCs) are discerned at 90 K in FT spectra of YM210W(L). These overtones disappear in the 935 nm kinetics in the dry films of the mutants (Figures 3C and 5C) in parallel with complete disappearance of ET from P* to B_A monitored by the absence of the 1020 nm band formation in both mutants (see Figure 1A for YM210W). The presence in the hydrated RCs of the higher overtones (up to the seventh, Figure 3C, curve c) of these modes indicates that they are rotational in nature, as suggested earlier.[26] As mentioned in the Introduction, the gasphase rotation of HOH has three frequencies at about 20, 32, and 52 cm⁻¹.[26] In *Rb. sphaeroides* RCs the frequency at 32 cm⁻¹ and its overtones are shifted by the same factor (∼1.3) to lower values when HOH is replaced by a mixture of HOD and DOD.[26] Taken together, these data are consistent with involving a water molecule in the ET pathway between P* and B_A in accordance with earlier suggestions.[26] It might be possible therefore that ET from P* to B_A occurs in *Rb. sphaeroides* RCs via a bridge with polar groups ("molecular wire") between P and B_A: N−Mg(P_B)−N−C−N(His M202)−HOH55−O=(B_A), containing the water molecule at the position 55 (see Brookhaven Protein Data Bank, 1AIJ, Figure 7). Similar polar groups are also observed in the structure of the *R. viridis* RCs (Brookhaven Protein Data Bank, 1PRC). This assumption is consistent with theoretical calculations[46] showing that the maximum electron density in the state P* is located on nitrogen atoms of P_B close to the nitrogen of HisM202 ligating the Mg atom of P_B.

In the absence of the electron transfer from P* to B_A and of the rotational mode at 32 cm⁻¹ with its overtones in the dry film of the YM210W mutant, the vibrational mode at 144 cm⁻¹ is clearly revealed in the 935 nm kinetics with second and third overtones at 289 and 434 cm⁻¹, respectively (Figure 3C). This suggests that the 144 cm⁻¹ oscillation (probably vibrational) is activated inside the dimer P. It is independent of the presence of the water molecule and of tyrosine M210. Furthermore, the 144 cm⁻¹ oscillation and the excited state P* itself do not include the 1020 nm band formation. It is likely that the 144 cm⁻¹ oscillation induces the overtones (close in energy to the mode at 144 cm⁻¹) of HOH rotational modes at 32 and 52 cm⁻¹ in the hydrated native and pheophytin-modified[21,26] or mutant YM210W and YM210L RCs observed in the 935 nm kinetics (Figures 3C and 5C). The fundamental frequency at 32 cm⁻¹ itself (period of ∼1 ps) is clearly observed in the 1020 nm kinetics when the stabilization of $P^+B_A^-$ occurs within 1.5 ps in pheophytin-modified (Figure 2A,B) and native RCs at 90 K[26] or within 3 ps in native (Figure 6A,B, curves b) and Pheo-modified RCs at 293 K.[21] This probably means that within 1−3 ps the stabilization process induces relatively slow water molecule rotation at 32 cm⁻¹ that modulates ET occurring via the above-mentioned bridge (see below).

Summarizing the data discussed above, one can see from Figure 3B,C that in the dry film of YM210W RCs only vibrational oscillation with a frequency of 144 cm⁻¹ is observed inside of P*. No rotational 32 cm⁻¹ mode and its overtones are discerned (Figure 3C) and no ET from P* to B_A occurs (Figure 1). From the X-ray model (Figure 7) one can conclude that in this case the vibrations are limited only by P molecules and possibly by HisM202 and HisL173 molecules and amino acids at M210 (see below). In hydrated YM210W mutant the overtones of the 31 cm⁻¹ mode are slightly discerned on the background of the 144 cm⁻¹ mode (Figures 2 and 3). These overtones and appearance of the limited reversible ET from P* to B_A monitored by 1020 nm band formation (Figure 2) seem to show some involvement of the molecules HOH55 and B_A in oscillations which are accompanied by ET from P* via HOH to B_A (Figure 7). However, the dominant 32 cm⁻¹ overtones in FT spectrum (Figure 3C, curves c) and maximum amplitude of ET from P* to B_A (monitored at 1020 nm, Figure 2, curves b) in pheophytin-modified RCs demonstrate the optimized coupling between nuclear motions (involving P*, HOH55 and B_A) and ET from P* to B_A in the complete system.

An important aspect of the charge separation between P* and B_A is related to the mechanism of stabilization of the separated charges in the state $P^+B_A^-$, which is characterized by a quasi-exponential rise of the level of $P^+B_A^-$ and decay of P* in the picosecond time domain in native and pheophytin-modified RCs.[21,26] Such stabilization clearly observed for pheophytin-modified (Figure 2, curves b and Figure 3, curves c) and for native RCs (Figure 6, curves b) is considerably suppressed in the mutants YM210W and YM210L (Figures 2 and 3, curves a; Figures 4 and 5). A reason for it can be related to the rising energy of $P^+B_A^-$, which is slightly higher than that of P* in the mutants.[39] However, even in this case the reversible fs ET from P* to B_A is clearly seen in the 1020 nm kinetics of the mutants (Figure 2, curves a, and Figure 4). This implies that the wave packet energy is enough to approach the intercrossing area between the P* and $P^+B_A^-$ surfaces but is not sufficient to provide a stabilization of $P^+B_A^-$ in the mutants.

Let us consider some details of the mechanism of the dynamic stabilization of $P^+B_A^-$ in RCs. Two possibilities should be considered. One of them is that an electron from P* can be transferred to the higher vibrational level on the $P^+B_A^-$ potential energy surface with subsequent vibrational relaxation to the lowest level according to well-known standard ET theory (see ref 20 for references therein). This possibility requires a

8336 *J. Phys. Chem. A, Vol. 107, No. 40, 2003*

Yakovlev et al.

nonsymmetrical arrangement of the potential energy surfaces of P* and $P^+B_A^-$ with ΔG around -500 cm^{-1}.[47,48] As a result, a relatively slow ET from P* to B_A might occur. According to this theory in the mutants YM210W and YM210L the ΔG value rises to zero or a slightly positive value, thus blocking the stabilization of separated charges. It was shown that in *C. aurantiacus* RCs, ET from P* to bacteriopheophytin located in the B-branch close to P occurs at 90 K with the amplitude less than 6% of the maximum value observed for ET to H_A in the A-branch.[49] Because ΔG for this reaction should be negative, this finding seems to represent an example of ET according to standard theory.

Another possibility is that stabilization of $P^+B_A^-$ can be due to a reorientation of surrounding groups when $P^+B_A^-$ is reversibly formed. In this case the symmetrical arrangement of the P* and $P^+B_A^-$ surfaces is possible with the maximum rate of reversible ET from P* to B_A. When the nuclear wave packet on the P* surface approaches the intercrossing area between two surfaces, both states (P* and $P^+B_A^-$) are registered (Figures 2–5). The wave packet goes back and forth between the P* and $P^+B_A^-$ surfaces if there is no additional noncoherent change in the nuclear position. This seems to be observed in the mutants YM210W and YM210L having slowly decaying fs oscillations in the formation of $P^+B_A^-$ (Figures 2–5). However, the nuclear position can be noncoherently changed by reorientation of the surrounding polar group like $O^{\delta-}H^{\delta+}$ of TyrM210 in native or Pheo-modified RCs (Figure 7). Then the motion of $H^{\delta+}$ toward B_A^- could lower the energy of $P^+B_A^-$ with respect to that of P* and stabilize $P^+B_A^-$. The estimation of the Coulomb energy changes (ΔE) in the system was done using the following expression:

$$\Delta E = e^2/\epsilon \sum_{i,j} \gamma_{i,j}/r_{ij} \qquad (1)$$

where e is an elementary charge, $\gamma_{i,j}$ are coefficients for electron density on corresponding atoms, ϵ is a dielectric constant of the media, and r_{ij} are distances between atoms. The estimations were done for two positions of $H^{\delta+}$ of OH-TyrM210 with respect to P_A and B_A having mostly positive and negative charges, respectively, in the state $P^+B_A^-$.[46] In the first ("neutral") position, a dipole $O^{\delta-}H^{\delta+}$ of TyrM210 is perpendicular to a line running between C–N(IV) of P_A and N(II) of B_A, which are the closest neighbors to TyrM210 and mostly populated by positive and negative charges, respectively, in the state $P^+B_A^-$.[46] This position on average was suggested to be realized in the neutral states PB_A or P^*B_A, thus giving Coulomb interaction close to zero. Even for the state $P^+B_A^-$ the Coulomb interaction is not significant (several wavenumbers). In the second position, $H^{\delta+}$ of OH-TyrM210 is on a line connecting $O^{\delta-}$ of OH-TyrM210 and N(II) of B_A. This position is assumed to occur when $P^+B_A^-$ is stabilized due to motion of $H^{\delta+}$ toward B_A attracted to and repulsed by B_A^- and P_A^+, respectively, in the state $P^+B_A^-$. The Coulomb energy interaction of P_A^+ and B_A^- with $O^{\delta-}$ and $H^{\delta+}$ for the second position was estimated to be ~840 cm^{-1}: 260 cm^{-1} for interaction with P_A^+, and 580 cm^{-1} for interaction with B_A^-. The experimental energy difference between P* and $P^+B_A^-$ in the stabilized state $P^+B_A^-$ in Pheo-modified RCs was found to be 350–550 cm^{-1}.[47,48] To get isoenergetic positions of two energy surfaces P* and $P^+B_A^-$ during the primary charge separation, the $H^{\delta+}$ position might be between the first and second positions described above.

The following shows the estimation of the time of a shift of $H^{\delta+}$ from the first to the second position due Coulomb attraction and repulsion of $H^{\delta+}$ by charged atoms of B_A^- and P_A^+,

respectively, separated by distances r_{ij}. During time t (~100 fs) of each appearance of the wave packet between the P* and $P^+B_A^-$ surfaces the distance (s) covered by $H^{\delta+}$ was estimated by means of the following expression:

$$s = t^2/2 \sum_{i,j} e^2 \gamma_{i,j}/(\epsilon r_{ij}^2 m) \qquad (2)$$

where m is the mass of H. The estimation demonstrates that in 65% of RCs an electron is stabilized on B_A (due to a shift of $H^{\delta+}$ from the first to second position) at approximately the fifth peak of fs oscillations at ~1 ps (τ_e) and 0 K. This is consistent with earlier data on the P* lifetime measurements at 10 K[18] and with Figures 2 (curves b) and 3 (curves c).

The reasonable coincidence of estimation and measurements seems to support the suggestion that the stabilization of $P^+B_A^-$ is provided by the reorientation of $H^{\delta+}$ of OH-TyrM210 and coherent ET from P* to B_A. It is important that the attraction and repulsion of $H^{\delta+}$ of OH-TyrM210 by B_A^- and P_A^+, respectively, occur when $P^+B_A^-$ is formed and are absent in the neutral state P*. The increase of the stabilization time with temperature[18] is consistent with the suggested mechanism because the interaction of $H^{\delta+}$ of OH-TyrM210 with phonons can produce some additional $H^{\delta+}$ motions leading to an increase of the stabilization time. The observation of the 32 cm^{-1} oscillation during the stabilization process in native or Pheo-modified RCs (Figures 2 and 6) might indicate some connection between the $H^{\delta+}$ motion of TyrM210 and the HOH rotation with a period of ~1 ps.

It is possible that the stabilization of $P^+B_A^-$ observed in *C. aurantiacus* RCs (Figure 6A) is due to the presence of TyrM195 located between P and B_A. The stabilization takes a longer time (~5 ps) at 90 K than in R-26 RCs (1.5 ps). This can be related to a nonsymmetrical position of TyrM195 with respect to P_A and B_A (in contrast to that for TyrM210 (Figure 7)) and/or to the relatively low amplitude of fs oscillations for the $P^+B_A^-$ formation in *C. aurantiacus* RCs. Interestingly, in *Rps. viridis* RCs both TyrM208 and TyrM195 are present. The rate of the charge stabilization in *Rps. viridis* RCs is a maximum at low temperature (1/0.8 ps[18]) and close to a sum of the charge stabilization rates in *Rb. sphaeroides* (1/1.2 ps[18]) and in *C. aurantiacus* (1/5 ps) RCs.

The kinetic data obtained for *C. aurantiacus* RCs at 90 K show (Figure 6) fs oscillations with FT spectra including the mode (probably vibrational) around 160 cm^{-1} and modes at 35 and 52 cm^{-1} with their overtones at 72, 109, and 176 cm^{-1} probably related to HOH rotation as well. However, there are no structural data supporting this suggestion. The FT spectrum for *C. aurantiacus* can be compared with that observed for YM210L(W) of *Rb. sphaeroides* in some respect. The spectrum in *C. aurantiacus* shows that the leucine at position M210 appears to induce not only a vibrational mode near 160 cm^{-1} but some additional vibrational mode near 110 cm^{-1} (Figure 6C), which is evidently observed in the dry film of YM210L RCs (Figure 5C) but not in that of YM210W where only the mode at 144 cm^{-1} is discerned (Figure 3C). This is consistent with measurements in dry film of *C. aurantiacus* RCs, which show two vibrational modes (not shown). On the other hand, the tyrosine at position M210 induces the mode at 122 cm^{-1} seen in dry films of pheophytin-modified RCs,[26] which is between the 110 and 144 cm^{-1} modes seen in YM210L (both modes) and YM210W (144 cm^{-1} mode) dry films. These data indicate the interaction between P* and amino acid at the position M210 in formation of vibrational modes of P*, in agreement with earlier data.[38] This finding might be consistent

Separated Charges in *C. aurantiacus* and *Rb. sphaeroides*

J. Phys. Chem. A, Vol. 107, No. 40, 2003 **8337**

with the relatively short distance (3.4 Å) between the oxygen of the acetyl group of ring I of P_B and the oxygen of TyrM210 (Brookhaven Protein Data Bank, 1AIJ).

The decrease of the initial amplitude of fs oscillations of the 1020−1028 nm band by a factor of ∼6−10 in the YM210W-(L) mutants of *Rb. sphaeroides* and in *C. aurantiacus* RCs with respect to native and Pheo-modified R-26 RCs is of interest for further discussion (see also ref 51). The reason for it seems to be related to the absence of tyrosine at the position M208 in *C. aurantiacus* RCs (LM208) and in YM210W(L) of *Rb. sphaeroides*. If $H^{\delta+}$ of OH-TyrM210 in *Rb. sphaeroides* is shifted toward B_A, it can lower the free energy of $P^+B_A^-$ with respect to P*. In the absence of TyrM210 in mutant RCs the energy of $P^+B_A^-$ may be above that of P*, as suggested earlier.[38,39] On the other hand, the positive shift of the redox potential of P/P$^+$ is equal to 55 mV (∼440 cm^{-1}) for YM210W and only 31 mV (∼250 cm^{-1}) for YM210L with respect to native RCs.[50] Note that the last value is very close to that obtained for the estimation of the Coulomb interaction of OH-TyrM210 with P_A^+ (∼260 cm^{-1}) in the second position of H (see above). It would mean that in the presence of TyrM210 the redox potential of P/P$^+$ is lowered by 250 cm^{-1} with respect to YM210L due to the Coulomb interaction of P$^+$ and OH-TyrM210 with H in the second position (due to thermalization). In YM210W the redox potential is increased even more (440 cm^{-1}). In contrast to that difference, the initial amplitudes of the fs oscillations in the 1020 nm kinetics are similar for both mutants (Figures 2A and 4A). The value of 440 cm^{-1} is close to the energy difference between P* and $P^+B_A^-$ (350−550 cm^{-1} [47,48]). From these facts one can suggest that the wave packet energy (∼150 cm^{-1} [26]) is slightly above (at least by ∼50 mV) the intercrossing point between the P* and $P^+B_A^-$ potential surfaces in the YM210W mutant. But the wave packet energy should be even higher than the intercrossing point energy for YM210L. In other words, the free energy of $P^+B_A^-$ can be lower than that of P* by ≥90 cm^{-1} in YM210L. This is enough to get some stabilization of $P^+B_A^-$ at 90 K (∼60 cm^{-1}). This is consistent with an appearance of the slight stabilization of $P^+B_A^-$ in YM210L (Figure 4A) in contrast to YM210W for which the stabilization is almost absent (Figure 2A). Note that the stabilization in YM210L is very slow (Figure 4A), supporting the assumption about the role of Tyr M210 in this process. In *C. aurantiacus* RCs the redox potential of P/P$^+$ is lower by 70−90 mV (560−720 cm^{-1}) than that in *Rb. sphaeroides*.[30,31] Therefore the reason for the small amplitude of fs oscillations in YM210 mutant of *Rb. sphaeroides* and in *C. aurantiacus* RCs is not simply mutual energy positions of the P* and $P^+B_A^-$ surfaces.

The tyrosine at the position M210 in *Rb. sphaeroides* seems to be responsible for the high fs oscillation amplitude, due not simply to lowering the energy level of $P^+B_A^-$ with respect to P* in the dark. Figure 7 and atomic coordinates of 1AIJ (Brookhaven Protein Data bank) show that the distances between atoms H−O−(TyrM210) and N−(HisM202), O−(HOH55), O−(keto group of ring V of B_A), and N(II)−(B_A) are different. Estimations using expression 1 show that the interaction energy of $H^{\delta+}O^{\delta-}$ of TyrM210 in the first position of H (see above) with atoms having an electron due to charge separation such as O$^-$−(HOH55) and both N$^-$−(HisM202) lies in the range of 280 cm^{-1}. In contrast, the interaction energy with O−(keto group of ring V of B_A) is greater (∼580 cm^{-1}). In other words, the first position of OH−YM210 is probably optimal for the relatively high amplitude of the fs oscillation of the electron density between P* and B_A via a "molecular wire" connecting

P and B_A. In the absence of TyrM210 the energy levels of all intermediate states should be increased but less for interaction with O$^-$−HOH55 and both N$^-$−HisM202 (∼280 cm^{-1}) and much more for interaction with O$^-$−B_A (∼580 cm^{-1}). As a result, even for *C. aurantiacus* the increase of the energy level of P* does not completely improve the situation because an electron has some energy barrier (∼300 cm^{-1}) on the last steps of ET from P* to B_A. This could partially explain the low amplitude of the fs oscillations at 1020−1028 nm in mutants YM210W(L) of *Rb. sphaeroides* and even in *C. aurantiacus* RCs.

References and Notes

(1) Michel, H.; Epp, O.; Deisenhofer, J. *EMBO J.* **1986**, *5*, 2445−2451.

(2) Komiya, H.; Yeates, T. O.; Rees, D. C.; Allen, J. P.; Feher, G. *Proc. Natl. Acad. Sci. U.S.A.* **1988**, *85*, 9012−9016.

(3) Maroti, P.; Kirmaier, C.; Wraight, C.; Holten, D.; Pearlstein, R. M. *Biochim. Biophys. Acta* **1985**, *810*, 132−141.

(4) Shuvalov, V. A.; Klevanik, A. V.; Sharkov, A. V.; Matveetz, Yu. A.; Krukov, P. G. *FEBS Lett.* **1978**, *91*, 135−139.

(5) Arlt, T.; Schmidt, S.; Kaiser, W.; Lauterwasser, C.; Meyer, M., Scheer, H.; Zinth, W. *Proc. Natl. Acad. Sci. U.S.A.* **1993**, *90*, 11757−11761.

(6) Shkuropatov, A. Ya.; Shuvalov, V. A. *FEBS Lett.* **1993**, *322*, 168−172.

(7) Schmidt, S.; Arlt, T.; Hamm, P.; Huber, H.; Nagele, T.; Wachtveitl, J.; Meyer, M.; Scheer H.; Zinth, W. *Chem. Phys. Lett.* **1994**, *223*, 116−120.

(8) Schmidt, S.; Arlt, T.; Hamm, P.; Huber, H.; Nagele, T.; Wachtveitl, J.; Zinth, W.; Meyer, M.; Scheer H. *Spectrochim. Acta, Part A* **1995**, *51*, 1565−1578.

(9) Kennis, J. T. M.; Shkuropatov, A. Ya.; Van Stokkum, I. H. M.; Gast, P.; Hoff, A. J.; Shuvalov, V. A.; Aartsma, T. J. *Biochemistry* **1997**, *36*, 16231−16238.

(10) Arlt, T.; Dohse, B.; Schmidt, S.; Wachtveitl, J.; Laussermair, E.; Zinth, W.; Oesterhelt, D. *Biochemistry* **1996**, *35*, 9235−9244.

(11) Spörlein, S.; Zinth, W.; Watchtveitl, J. *J. Phys. Chem. B* **1998**, *102*, 7492−7496.

(12) Spörlein, S.; Zinth, W.; Meyer, M.; Scheer, H.; Watchtveitl, J. *Chem. Phys. Lett.* **2000**, *322*, 454−464.

(13) Beekman, L. M. P. Ph.D. Thesis (promoter, R. van Grondelle), VU, Amsterdam, 1997.

(14) Marcus, R. A. In *The Photosynthetic Bacterial Reaction center: Structure and Dynamics*; Breton, J., Vermeglio, A., Eds.; Plenum Press: New York, London, 1989; pp 389−398.

(15) Bixon, M.; Jortner, J. *J. Phys. Chem.* **1986**, *90*, 3795−3800.

(16) Kitzing, E.; Kuhn, H. *J. Phys. Chem.* **1990**, *94*, 1699−1715.

(17) Parson, W. W.; Warshel, A. *J. Am. Chem. Soc.* **1987**, *109*, 6152−6163.

(18) Fleming, G. R.; Martin, J.-L.; Breton, J. *Nature (London)* **1988**, *333*, 190−192.

(19) Larsson, S.; Ivashin, N. V. *J. Appl. Spectrosc.* **1999**, *66*, 539−543.

(20) Bixon, M.; Jortner, J.; Plato, M.; Michel-Beyerle, M. E. In *The Photosynthetic Bacterial Reaction center: Structure and Dynamics*; Breton, J., Vermeglio, A., Eds.; Plenum Press: New York, London, 1988; pp 399−419.

(21) Yakovlev, A. G.; Shkuropatov, A. Ya.; Shuvalov, V. A. *Biochemistry* **2002**, *41*, 2667−2674.

(22) Vos, M. H.; Rappaport, F.; Lambry, J.-C.; Breton, J.; Martin, J.-L. *Nature* **1993**, *363*, 320−325.

(23) Vos, M. H.; Jones, M. R.; McGlynn, P.; Hunter, C. N.; Breton, J.; Martin, J.-L. *Biochim. Biophys. Acta* **1994**, *1186*, 117−122.

(24) Vos, M. H.; Jones, M. R.; Hunter, C. N.; Breton, J.; Lambry, J.-C.; Martin, J.-L. *Biochemistry* **1994**, *33*, 6750−6757.

(25) Vos, M. H.; Rischel, C.; Jones, M. R.; Martin, J.-L. *Biochemistry* **2000**, *39*, 8353−8361.

(26) Yakovlev, A. G.; Shkuropatov, A. Ya.; Shuvalov, V. A. *Biochemistry* **2002**, *41*, 14019−14027.

(27) Streltsov, A. M.; Vulto, S. I. E.; Shkuropatov, A. Ya.; Hoff, A. J.; Aartsma, T. J.; Shuvalov, V. A. *J. Phys. Chem. B* **1998**, *102*, 7293−7298.

(28) Yakovlev, A. G.; Shkuropatov, A. Ya.; Shuvalov, V. A. *FEBS Lett.* **2000**, *466*, 209−212.

(29) Yakovlev, A. G.; Shuvalov, V. A. *J. Chin. Chem. Soc.* **2000**, *47*, 709−714.

(30) Shuvalov, V. A.; Shkuropatov, A. Y.; Kulakova, S. M.; Ismailov, M. A.; Shkuropatova, V. A. *Biochim. Biophys. Acta* **1986**, *849*, 337−348.

(31) Bruce, B. D.; Fuller, R. C.; Blankenship, R. E. *Proc. Natl. Acad. Sci. U. S.A.* **1982**, *79*, 6532−6536.

(32) Shuvalov, V. A.; Vasmel, H.; Amesz, J.; Duysens, L. N. M. *Biochim. Biophys. Acta* **1986**, *851*, 361−368.

(33) Feick, R.; Martin, J.-L.; Breton, J.; Volk, M.; Landenbacher, T.; Urbano, C.; Ogrodnik, A.; Michel-Beyerle, M. E. In *Reaction Centers of Photosynthetic Bacteria*; Michel-Beyerle, M. E., Ed.; Springer-Verlag: Berlin, 1990; pp 181−188.

(34) Becker, M.; Nagarajan, V.; Middendorf, D.; Parson, W. W.; Martin, J. E.; Blankenship, R. E. *Biochim. Biophys. Acta* **1991**, *1057*, 299−312.

(35) Hamm, P.; Gray, K. A.; Oesterhelt, D.; Feick, R.; Scheer, H.; Zinth, W. *Biochim. Biophys. Acta* **1993**, *1142*, 99−105.

(36) Hastings, G.; Lin, S.; Zhou, W.; Blankenship, R. E. *Photochem. Photobiol.* **1993**, *57*, 65.

(37) Feick, R.; Shiozawa, J. A.; Ertlmaier, A. In *Anoxygenic Photosynthetic Bacteria*; Blankenship, R. E., Madigan, M. T., Bauer, C. E. Eds.; Kluwer Academic Publishers: The Netherlands, 1995; pp 699−708.

(38) Vos, M. H.; Jones, M. R.; Breton, J.; Lambry, J.-C.; Martin, J.-L. *Biochemistry* **1996**, *35*, 2687−2692.

(39) Nagarajan, V.; Parson, W. W.; Davis, D.; Schenck, C. *Biochemistry* **1993**, *32*, 12324−12336.

(40) Jia, Y.; DiMagno, T. J.; Chan, C.-K.; Wang, Z.; Du, M.; Hanson, D. K.; Schiffer, M.; Norris, J. R.; Fleming, G. R.; Popov, M. S. *J. Phys. Chem.* **1993**, *97*, 13180−13191.

(41) Shochat, S.; Arlt, T.; Francke, C.; Gast, P.; Van Noort, P. I.; Otte, S. C. M.; Schelvis, H. P. M.; Schmidt, S.; Vijgenboom, E.; Vrieze, J.; Zinth, W.; Hoff, A. J. *Photosynth. Res.* **1994**, *40*, 55−66.

(42) Beekman, L. M. P.; Van Stokkum, I. H. M.; Monshouwer, R.; Rijnders, A. J.; McGlynn, P.; Visschers, R. W.; Jones, M. R.; Van Grondelle, R. *J. Phys. Chem.* **1996**, *100*, 7256−7268.

(43) McAuley, K. E.; Fyfe, P. K.; Cogdell, R. J.; Isaacs, N. W.; Jones, M. R. *FEBS Lett.* **2000**, *467*, 285−290.

(44) Vasilieva, L. G.; Bolgarina, T. I.; Khatypov, R. A.; Shkuropatov, A. Ya.; Shuvalov, V. A. *Dokl. Acad. Nauk. (Russian)* **2001**, *376*, 826−829.

(45) Franken, E. M.; Shkuropatov, A. Ya.; Francke, C.; Neerken, S.; Gast, P.; Shuvalov, V. A.; Hoff, A. J.; Aartsma, T. J. *Biochim. Biophys. Acta* **1997**, *1321*, 1−9.

(46) Plato, M.; Lendzian, F.; Lubitz, W.; Trankle, E.; Mobius, K. In *The Photosynthetic Bacterial Reaction Center: Structure and Dynamics*; Breton, J., Vermeglio, A., Eds.; Plenum Press: New York, London, 1988; pp 379−388.

(47) Shuvalov, V. A.; Yakovlev, A. G. *Membr. Cell Biol.* **1998**, *12*, 563−569.

(48) Nowak, F. R.; Kennis, J. T. M.; Franken, E. M.; Shkuropatov, A. Ya.; Yakovlev, A. G.; Gast, P.; Hoff, A. J.; Aartsma, T. J.; Shuvalov, V. A. *Proceedings of the XIth International Congress on Photosynthesis*, Budapest, Hungary; Kluwer Academic Publishers: Dordrecht, The Netherlands, 1998; pp 783−786.

(49) Shuvalov, V. A.; Yakovlev, A. G. *FEBS Lett.* **2003**, *540*, 26−34.

(50) Beekman, L. M. P.; van Stokkum, I. H. M.; Monshouwer, R.; Rijnders, A. J.; McGlynn, P.; Visschers, R. W.; Jones, M. R.; van Grondell, R. *J. Phys. Chem.* **1996**, *100*, 7256−7268.

(51) Wachtveitl, J.; Huber, H.; Feik, R.; Rautter, J.; Muh, F.; Lubitz, W. *Spectrochim. Acta, Part A* **1998**, *54*, 1231−1245.